BOLETIN LATINOAMERICANO Y DEL CARIBE DE PLANTAS MEDICINALES Y AROMÁTICAS
© / ISSN 0717 7917 / www.blacpma.ms-editions.cl

Articulo Original / Original Article

Effects of Yishentongluo Recipe on Nrf2 and HO-1 pathway activation leading to reduction of oxidative stress and kidney fibrosis in membranous nephropathy rat model

[Efectos de la receta de Yishentongluo sobre la activación de las vías Nrf2 y HO-1 que conducen a la reducción del estrés oxidativo y fibrosis renal en un modelo de rata con nefropatía membranosa]

Guo-Dong Yuan[1], Ze-Ze Wang[2], Ming-Xin Guo[3], Yu-Chuan He[3], Yuan-Hang Liu[4] & Jin-Chuan Tan[1]

[1]Department of Nephrology 1, Hebei Hospital of Traditional Chinese Medicine, Shijiazhuang, China
[2]Shijiazhuang Traditional Chinese Medicine Hospital, Shijiazhuang, China
[3]Graduate School of Hebei University of Traditional Chinese Medicine, Shijiazhuang, China
[4]Tianjin University of Traditional Chinese Medicine, Tianjin, China

Reviewed by:
Miguel Moreno
Universidad de San Salvador
El Salvador

Rafael Mex Alvarez
Universidad Autonoma de Campeche
Mexico

Correspondence:
Jin-Chuan TAN
tanjinchuanaug@126.com

Section Biotechnology

Received: 29 June 2023
Accepted: 29 January 2023
Accepted corrected: 27 March 2024
Published: 30 September 2024

Citation:
Yuan GD, Wang ZZ, Guo MX, He YC, Liu YH, Tan JC
Effects of Yishentongluo Recipe on Nrf2 and HO-1 pathway activation leading to reduction of oxidative stress and kidney fibrosis in membranous nephropathy rat model
Bol Latinoam Caribe Plant Med Aromat
23 (5): 783 - 792 (2024)
https://doi.org/10.37360/blacpma.24.23.5.50

Abstract: This study investigated Yishentongluo Recipe (YSTLF) effects on renal oxidative stress and fibrosis in membranous nephropathy (MN) rats. MN was induced by cationized bovine serum albumin injection. Rats were divided into control, MN, YSTLF, and benazepril groups. After four weeks of treatment, urine protein levels (UTP), serum total cholesterol (TC), triglycerides (TG), total protein (TP), and albumin (ALB) were assessed. Kidney microstructure, IgG immune complex deposition, and protein expressions of superoxide dismutase (SOD), malondialdehyde (MDA), transforming growth factor β1 (TGF-β1), collagen I (Collagen-I), α-smooth muscle actin (α-SMA), nuclear factor E2-related factor (Nrf2), haem oxygenase 1 (HO-1), and NADPH oxidase 4 (NOX4) were evaluated. YSTLF and BNPL treatments reduced UTP, TC, TG, increased TP and ALB levels, downregulated TGF-β1, Collagen-I, and α-SMA, and upregulated Nrf2, HO-1, and NOX4. YSTLF partially reversed SOD reduction and MDA elevation, suggesting its efficacy in alleviating renal oxidative stress and fibrosis in MN rats via Nrf2/HO-1 signaling pathway activation.

Keywords: Membranous nephropathy; Nrf2/HO-1; Oxidative stress; Renal fibrosis; Yishentongluo Recipe

Resumen: Este estudio investigó los efectos de la receta Yishentongluo (YSTLF) sobre el estrés oxidativo renal y la fibrosis en ratas con nefropatía membranosa (MN). La MN se indujo mediante inyección de albúmina sérica bovina cationizada. Las ratas se dividieron en grupos de control, MN, YSTLF y benazepril. Después de cuatro semanas de tratamiento, se evaluaron los niveles de proteína en orina (UTP), colesterol total (CT), triglicéridos (TG), proteína total (TP) y albúmina (ALB) en suero. Se evaluaron la microestructura renal, el depósito de complejos inmunes IgG y expresiones proteicas de superóxido dismutasa (SOD), malondialdehído (MDA), factor de crecimiento transformante β1 (TGF-β1), colágeno I (Colágeno-I), α-actina del músculo liso (α-SMA), el factor nuclear E2 (Nrf2), la hemooxigenasa 1 (HO-1) y la NADPH oxidasa 4 (NOX4). Los tratamientos con YSTLF y BNPL redujeron UTP, TC, TG, aumentaron los niveles de TP y ALB, regularon negativamente TGF-β1, Colágeno-I y α-SMA, y regularon positivamente Nrf2, HO-1 y NOX4. YSTLF revirtió parcialmente la reducción de SOD y la elevación de MDA, lo que sugiere su eficacia para aliviar el estrés oxidativo renal y la fibrosis en ratas MN mediante la activación de la vía de señalización Nrf2/HO-1.

Palabras clave: Nefropatía membranosa; Nrf2/HO-1; Estrés oxidativo; Fibrosis renal; Receta Yishentongluo

INTRODUCTION

Immunofluorescence imaging of a renal tissue biopsy allows for the definitive diagnosis of membranous nephropathy (MN), the most common primary kidney condition. This is achieved by identifying diagnostic features such as the presence of IgG and C3 complement deposits, thickening of the glomerular basement membrane, and the presence or absence of spike-like projections. The likelihood of the patient developing nephrotic syndrome (van de Logt *et al*., 2019) ranges from 40% to 75%. Approximately 30% of patients with MN experience spontaneous remission (Ronco *et al*., 2021), while 30% to 50% may progress to end-stage renal disease (Beck & Salant, 2014). Renal fibrosis, a degenerative change where normal kidney tissue is replaced by extracellular matrix (ECM), can be triggered by the ongoing development of various primary or secondary renal disorders. This gradual and irreversible damage to renal functions ultimately leads to end-stage renal failure.

ECM formation and accumulation can be stimulated while also being inhibited by TGF-1 and collagen-I, which are important factors in fibrosis. As a result, this mechanism interferes with the division and expansion of tubular and glomerular epithelial cells, resulting in interstitial fibrosis and glomerulosclerosis. They also have a strong stimulating effect on the production and accumulation of ECM, which is essential for controlling the metabolism of ECM and promoting the development of renal interstitial fibrosis (Zhang *et al*., 2020).

MN mostly develops due to glomerular podocyte destruction. Podocytes may be destroyed and undergo apoptosis due to oxidative damage and endoplasmic reticulum stress (Lei & He, 2019). A surplus of reactive oxygen species (ROS) produced by cells can also promote cell growth, improve the glomerular ECM, thicken the glomerular basement membrane, and cause glomerular hypertrophy, sclerosis, and subsequently renal fibrosis. Antioxidant stress genes are activated by a major transcription factor known as nuclear factor erythrocyte 2-related factor (Nrf2). Nrf2 can efficiently counteract oxidative stress by boosting the production of heme oxygenase-1(HO-1), glutamate-cysteine ligase (GCLC), and quinone oxidoreductase-1 (NQO-1) (Li *et al*., 2017). A traditional Chinese medicine called Yishentongluo Recipe is used to treat MN. It seeks to "achieve balance by adjusting the normal treatment and removing accumulation". This formula has a clear etiology, specific ingredients, and has demonstrated acceptable clinical efficacy in the treatment of MN. The purpose of this study is to investigate the effects and possible mechanisms of Yishentongluo Recipe (YSTLF) on renal fibrosis and oxidative stress in rats with MN. The findings are intended to offer strong evidence to support its use in clinical practice.

MATERIALS AND METHODS

Animals

Age matched 8 week - old male clean-grade healthy male SD rats (150 ± 20 g) were involved in this experiment, which were obtained from the Animal Experiment Center of Hebei Medical University, with the Animal Certificate No. 1904033. The Laboratory Animal License No. was SYXK (J) 2018-004.

Medicine

The Yishentongluo Recipe, provided by the Preparation Room of Hebei Provincial Hospital of Chinese Medicine, consists of a combination of Chinese medicinal ingredients. The recipe includes the following ingredients and their respective quantities: *Astragali radix* (20 g), *Codonopsis radix* (15 g), fried atractylodis macrocephalae rhizoma (15 g), *Epimedii folium* (15 g), *Gynostemma pentaphylla* (15 g), *Angelicae sinensis* radix (15 g), *Curcumae* rhizoma (12 g) processed with vinegar, Pheretima (12 g), and Hirudo (9 g). In the experiment, the decoction form of the Chinese medicines was used, and the equivalent conversion was made using formula granules provided by E-FONG Pharmaceutical. The approval numbers for the corresponding medicines are as follows: *Astragali radix* (9080243), *Codonopsis radix* (9080133), fried atractylodis macrocephalae rhizoma (9070353), *Epimedii folium* (8086043), *Gynostemma pentaphylla* (8105133), *Angelicae sinensis* radix (9065173), *Curcumae* rhizoma processed with vinegar (8091513), Pheretima (9025923), and Hirudo (9051103).

Reagents

Cationized bovine serum albumin (C-BSA) used in this experiment was purchased from Chondrex, Inc (Washington, USA). Freund's incomplete adjuvant were brought from Sigma (Missouri, USA). Besides, we obtained albumin assay kit, total protein quantitative assay kit (TP), Triglyceride assay kit (TG), total cholesterol assay kit (TC), urine protein test kit from Nanjing Jiancheng bioengineering institute (Nanjing, China). IgG fluorescent antibody and electron microscope fixative were obtained from INVITRONG (California, USA) and RedPartyTech

(Taiwan, China), respectively. The antibodies including β-actin, TGF-β1, Collagen-I, and α-SMA were brought from ABclonal Co., Ltd. (Wuhan, China). Additionally, we obtained antibodies including GAPDH, Nrf2, HO-1, and NOX4 antibodies from Affinity Inc. (USA).

Model preparation, grouping, and administration

A total of 44 male SD rats of clean grade and good health were bred under controlled conditions for one week with adjustable feeding. Once the urine protein test using test paper indicated negative results for urine proteins, 12 rats were randomly assigned to the normal control group (NC) Group, while the remaining 32 rats were assigned to the Modeling Group. The MN rat model was replicated by injecting C-BSA via the tail vein using the Border method (Border *et al*., 1982). To prepare the injection solution, 1 mg of C-BSA was combined with 0.5 mL of PBS and mixed with an equal amount of Freund's incomplete adjuvant until fully emulsified. A 1 mL emulsion was then injected into the axilla and groin of both forelimbs using sub-conjunctival injection. This procedure was repeated once every other day, three times a week, for a total of one week as part of the pre-immunization process.

Subsequently, every rat received formal immunization by means of an intravenous injection of C-BSA at a dosage of 16 mg/kg, three times per week, over a span of four weeks. Two rats were selected at random from the Modeling Group, while another two were chosen from the NC group. The results obtained from pathological staining and projection electron microscopy indicated the successful establishment of the MN rat model. Following the successful modeling process, the rats were randomly divided into three groups: the MN Group (administered 10 mL/kg), the benazepril (BNPL) Group (administered 10 mL/kg), and the YSTLF Group (administered 26.44 g/kg), with 10 rats allocated to each group. The rats in each group were given the corresponding volume of either the drug or distilled water once a day for a duration of four weeks.

Serum biochemistry test and 24 h urine protein quantification (UTP)

Following administration, urine was collected from the rats confined in the cage for a period of 24 hours. The volume of urine was recorded, and the liquid portion was subjected to centrifugation to determine the urinary total protein (UTP) levels. Subsequent to urine collection, each rat underwent anesthesia through intraperitoneal injection of 10% chloral hydrate, and the abdominal region was surgically opened. Approximately 5 mL of blood was obtained from the abdominal aorta and, after centrifugation, the serum was collected to assess various serum biochemical indicators, including TC, triglyceride (TG), total protein (TP), albumin (ALB), superoxide dismutase (SOD), and malondialdehyde (MDA).

Electron microscope observation of morphological structure of glomerular basement membrane and podocytes of the rats

About 1 mm^3 of rat renal cortex was extracted and was preserved in a 3% glutaraldehyde fixative at a temperature of 4°C for a duration of 1 hour. Afterwards, it was thoroughly cleansed using a phosphate buffer solution (PBS), followed by fixation using pre-cooled 1% osmium acid. After rinsing with PBS, the sample underwent a process of gradual dehydration using ethanol, embedding, polymerization, sectioning, and finally, it was subjected to double staining using uranyl acetate and lead citrate. Ultimately, observation and photography of the sample were carried out using a transmission electron microscope.

Immunofluorescence detection of IgG expression in rat renal cortex

The renal cortex of the rat was extracted and processed into 5 μm slices while kept on ice. These slices were then treated with cold acetone to fix them. To examine the level of glomerular IgG deposition, an indirect immunofluorescence technique was employed. FITC-labeled primary and secondary antibodies were carefully added for incubation. Once sealed with glycerol-phosphate buffer, the samples were observed and photographed under a microscope.

Detection of kidney-associated protein expression by western blot

The RIPA protein extraction reagent, supplemented with PMSF, was used to extract the total protein. The concentration of the protein was determined using the BCA method. A total of 50 μg of the protein was mixed with loading buffer and heated at 100°C for 5 minutes. Subsequently, a 10% SDS-PAGE gel was employed for electrophoresis at a constant voltage of 90 V for 2 to 3 hours. The PVDF transfer was performed at a constant current of 250 mA for 30 to 60 minutes. The PVDF membrane was then incubated in 5% BSA at 37°C for 1.5 hours. Primary antibodies, including β-actin (1:10,000), TGF-β1 (1:5,000), Collagen-I (1:4.000), α-SMA (1:3.000),

GAPDH (1:5.000), Nrf2 (1:4.000), HO-1 (1:3.000), and NOX4 (1:2.000), were added and allowed to incubate overnight at 4°C. Following membrane washing, the corresponding secondary antibody (1:5.000) was added and incubated at 37°C for 1 hour. After washing the membrane, the ECL method was used to develop the color, and the grayscale intensity of the bands was analyzed using Quantity One software. The ratio of the grayscale value of the target protein band to the β-actin (GAPDH) band was considered the final result.

Statistical analysis

Statistical analysis was performed using SPSS 21.0 software. Experimental data were expressed as mean ± standard deviation. When the data followed a normal distribution and had equal variances, an ANOVA analysis method following by the LSD test have been used for multiple comparisons. In cases when the data for a normal distribution were not met, the rank sum test was used instead. A *p*-value less than 0.05 ($p \leq 0.05$) indicated a statistically significant difference.

RESULTS

Effects of YSTLF on UTP in rats with MN, and serum TC, TG, TP, and ALB levels

After 4 weeks of continuous administration, compared with the MN Group, UTP and TC decreased significantly ($p<0.05$), while TP and ALB increased significantly ($p<0.05$) in the treatment groups (Table No. 1).

Table No. 1
Effects of Yishentongluo Recipe (YSTLF) on UTP and Serum TC, TP, and ALB Levels in Rats with MN (n=10)

Group	Dosage (g/kg)	UTP (mg/24h)	TC (mmol/L)	TG (g/L)	TP (g/L)	ALB (g/L)
NC Group	--	7.06 ± 0.53	1.09 ± 0.26	0.43 ± 0.06	56.79 ± 2.68	31.25 ± 1.64
MN Group	--	43.81 ± 1.62*	4.33 ± 0.52*	0.76 ± 0.08*	34.37 ± 2.14*	18.97 ± 1.33*
BNPL Group	0.01	28.67 ± 1.87#	2.45 ± 0.60#	0.59 ± 0.07#	43.84 ± 2.43#	24.44 ± 1.28#
YSTLF Group	13.22	25.04 ± 1.76#	2.02 ± 0.39#	0.48 ± 0.08#	47.68 ± 2.51#	24.61 ± 1.32#

Effects of YSTLF on pathological morphology of kidneys of rats with MN

The glomerular basement membrane and podocytes in rats from various groups were observed using an electron microscope. The glomerular basement membrane was not thickened in the NC Group, and the podocytes had clearly defined, orderly peduncles. The glomerular basement membrane of the renal tissue, however, was noticeably thicker in the MN Group, and there was a significant buildup of dense materials underneath the epithelium. Podocyte peduncles underwent significant fusion and finally disappeared.

The diseased structure of the podocytes and glomerular basement membrane in the rats improved to varied degrees in the MN Group compared to the YSTLF Group and BNPL Group. Comparing the two groups, the YSTLF Group showed more improvement than the BNPL Group (Figure No. 1).

Figure No. 1
Effects of Yishentongluo Recipe (YSTLF) on Pathological Morphology of Kidneys of Rats with membranous nephropathy (MN)
Note: A: NC Group; B: MN Group; C: YSTLF Group; D: BNPL Group

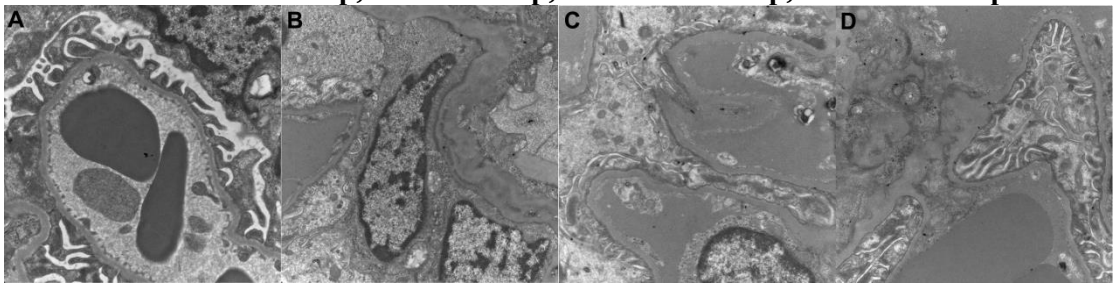

Effects of YSTLF on IgG deposition in kidney tissues of rats with MN

In the NC Group of rats, there was no IgG fluorescence deposition observed in kidney tissues. However, in the kidney tissues of rats belonging to the other groups, there were varying degrees of granular deposition of fluorescent IgG detected on the capillary wall. The fluorescence intensity was notably higher in the MN Group, whereas it was significantly weaker in the YSTLF Group and BNPL Group (Figure No. 2).

Figure No. 2
Effects of Yishentongluo Recipe (YSTLF) on IgG Deposition in Kidney Tissues of Rats with membranous nephropathy (MN)
Note: A: NC Group; B: MN Group; C: YSTLF Group; D: BNPL Group

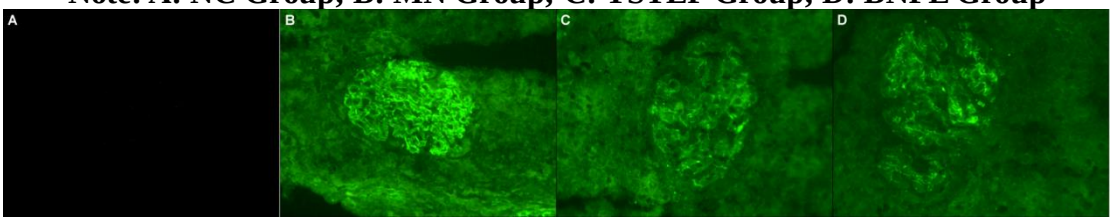

Effects of YSTLF on serum SOD and MDA in rats with MN

In comparison to the NC Group, the MN Group exhibited a decrease in SOD expression and an increase in MDA expression in rat serum (p<0.05). Conversely, when compared to the MN Group, the YSTLF Group and BNPL Group demonstrated an increase in SOD expression and a decrease in MDA expression in rat serum (p<0.05) (Table No. 2).

Table No. 2
Effects of Yishentongluo Recipe (YSTLF) on Serum SOD and MDA in Rats with MN

Group	Dosage (g/kg)	SOD(U/L)	MDA (nmol/mL)
NC Group	--	173.65 ± 8.17	5.63 ± 0.58
MN Group	--	148.34 ± 4.85*	8.87 ± 1.02*
BNPL Group	0.01	157.23 ± 5.09$^{\#}$	6.94 ± 0.53$^{\#}$
YSTLF Group	13.22	165.90 ± 5.34$^{\#}$	6.33 ± 0.51$^{\#}$

Effects of YSTLF on the expressions of TGF-β1, Collagen-I, and α-SMA in kidney tissues of rats with MN

In comparison to the NC Group, the levels of renal fibrosis markers TGF-β1, Collagen-I, and α-SMA were significantly higher in rats in the MN Group (p<0.05). On the other hand, the expressions of TGF-β1, Collagen-I, and α-SMA in rats in the YSTLF Group and BNPL Group showed a slight decrease when compared to the MN Group (p<0.05) (Figure No. 3).

Effects of expressions of Nrf2, HO-1, and NOX4 in kidney tissues of rats with MN

In comparison to the NC Group, the levels of Nrf2, HO-1, and NOX4 expressions in rat kidney tissues were higher in the MN Group, and these differences were statistically significant (p<0.05). This indicates that MN induced oxidative stress in the kidney and led to an increase in the compensatory anti-oxidative stress level. Moreover, when comparing the MN Group to the YSTLF Group and BNPL Group, the levels of Nrf2, HO-1, and NOX4 expressions in rat kidney tissues were also higher, and these differences were statistically significant (p<0.05) (Figure No. 4).

Figure No. 3
Effects of Yishentongluo Recipe (YSTLF) on Expressions of TGF-β1, Collagen-I, and α-SMA in Kidney Tissues of Rats with membranous nephropathy (MN)
Note: Upon Comparison with NC Group: *p<0.05; Upon comparison with MN Group: $^{\#}p$<0.05

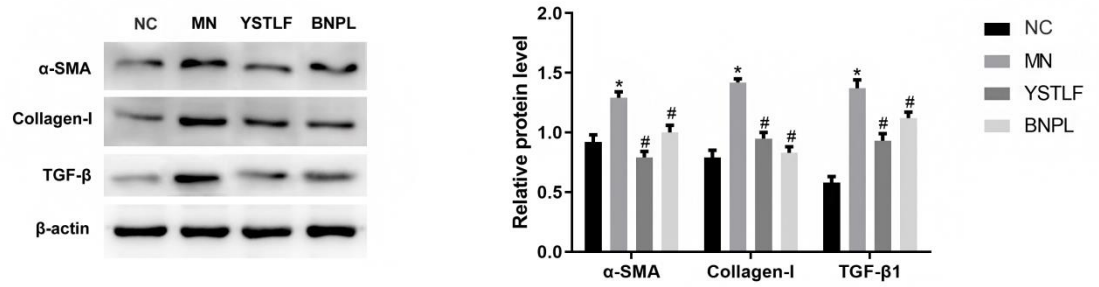

Figure No. 4
Effects of Yishentongluo Recipe (YSTLF) on Expressions of Nrf2, HO-1, and NOX4 in Kidney Tissues of Rats with membranous nephropathy (MN)
Note: Upon Comparison with NC Group: *p<0.05; Upon comparison with MN Group: $^{\#}p$<0.05

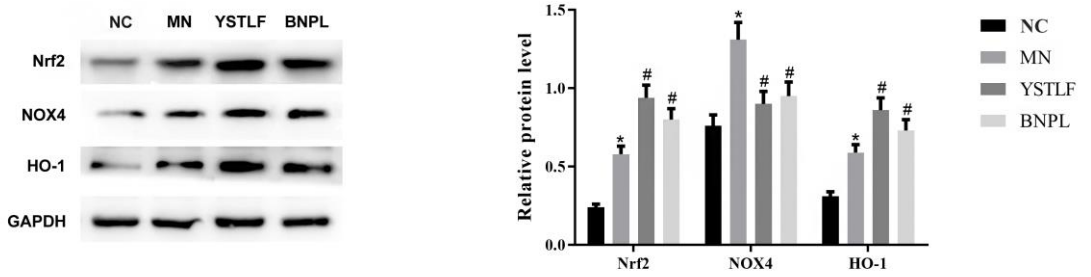

DISCUSSION

The occurrence of MN in China has been steadily increasing over the past few years. Typically, MN with medium-high risks is treated using hormones and immunosuppressive drugs. However, the potential complications like infection and liver damage have not received adequate attention. Therefore, it is important to discover new therapeutic approaches to further enhance treatment. To create an effective formula for clinical treatment of MN, the research team, led by Professor Zhao Yuyong, has conducted extensive clinical exploration and research based on their treatment experience. We believe that the root cause of MN lies in the deficiency of both the spleen and kidney, as well as blockage in the kidney channels. Building on this understanding, the YSTLF has been developed, which exhibits significant clinical effectiveness (Burbelo *et al*., 2020). Additionally, some progress has been made in related scientific research, and it is essential to investigate the potential mechanism behind the treatment of MN (Chen *et al*., 2018).

The YSTLF is composed of various herbs including *Astragali radix*, *Codonopsis radix*, fried atractylodis macrocephalae rhizoma, *Epimedii folium*, *Gynostemma pentaphylla*, *Angelicae sinensis* radix, *Curcumae* rhizoma, Pheretima, and Hirudo. The combination of *Astragali radix* and *Angelicae sinensis* radix, known as Danggui Buxue Decoction, is used to supplement qi and blood. Recent research indicates that this combination can inhibit renal fibrosis by suppressing the expression of TGF-β1. The alcohol-based extract of Astragali radix and Angelicae sinensis radix has been found to be more effective than the aqueous extract (Kim *et al*., 2018).

Astragali radix (Su *et al*., 2023), *Codonopsis* radix (Sun & Liu, 2008), fried atractylodis macrocephalae rhizome (Xie *et al*., 2013), and Epimedii folium (Sun *et al*., 2015; Chen *et al*., 2019; Sun *et al*., 2021), are tonic herbs that improve immunity and alleviate weakness in patients with kidney disease by tonifying the upper, middle, and

lower jiao, benefiting qi, invigorating the spleen, inducing diuresis, and clearing turbidity. The active components with the activities of improving immunity and alleviating weakness of these Chinese medicine were also given attentions by researchers. For instance, previous reports (Hoo *et al*., 2010; Li *et al*., 2022), have showed that the flavonoids of *Astragali* radix could performed renoprotection by improving immunity and energy metabolism. Besides, Gynostemma pentaphylla strengthens the stomach, aids digestion, relieves cough, resolves phlegm, clears heat, removes toxins, and improves intracellular oxidative stress levels. It also inhibits the proliferation of glomerular mesangial cells and the production and accumulation of ECM (Curthoys & Gstraunthaler, 2014; Wang *et al*., 2015; Wang *et al*., 2018).

Pheretima, Hirudo, and *Curcumae* rhizoma are drugs that promote blood circulation and alleviate blood stasis in kidney disease. Previous studies have found that the pathological state of blood stasis was also caused by dysfunctional microcirculation (Li *et al*., 2013; Yu & Wang, 2016), and often accompanied by a series of abnormalities (Lu *et al*., 2014; Ma *et al*., 2017; Yi *et al*., 2021; Chen *et al*., 2022), for example, the abnormality of hemodynamics, lipid/energy metabolite, the blood plasma viscosity, coagulation function as well as the inflammation injury. These accompanied abnormalities also suggested the potential pathological mechanism of blood stasis and the action mechanisms of therapeutic drugs, especially Chinese medicines. As the Chinese medicine for kidney disease with alleviating blood stasis efficacy, previous study showed that the beneficial effects of composite pheretima powder on diabetic nephropathy may be attributed to its high urokinase-type plasminogen activator like activity (Kawakami *et al*., 2016). Further studies also demonstrated that Pheretima and its active ingredients exhibited the bioactivity of repairing endothelial damage, stopping platelet aggregation, thwarting thrombosis, lowering cholesterol levels, strengthening immunity, and having antioxidant and anti-inflammatory effects (Gao *et al*., 2019), which may contribute to its efficacy on promoting blood circulation and alleviating the symptoms of blood stasis. In terms of Hirudo, one of the main drugs with alleviating blood stasis in YSTLF, the powder of it have been demonstrated to be used for regulating metabolic disorders, reducing oxidative damage, and inhibiting inflammatory responses by lowering lipid deposition in the body. Hirudo contains polypeptides that have anticoagulant and antithrombotic properties, reducing whole blood viscosity and plasma viscosity. Additionally, Hirudo secretes histamine-like substances that inhibit the increase in endothelin permeability (Li *et al*., 2019). These studies partly revealed the scientificity of the effects of Hirudo on alleviating blood stasis from the perspective of both chemical compound and potential mechanism. Similarly, the effects of *Curcumae* rhizoma on alleviate blood stasis also been reported by previous research, which may be partly related to its activities on decreasing in plasma viscosity, erythrocyte aggregation index as well as the erythrocyte sedimentation rate equation K value (Zhang *et al*., 2021). These above-mentioned researches provided some evidence support of the efficacies of Pheretima, Hirudo, and *Curcumae* rhizoma on promoting blood circulation and alleviating blood stasis.

The essential pathogenic mechanism of MN, which is defined by an imbalance between underlying inadequacies and outward excesses, was taken into account when developing the YSTLF. The purpose of this recipe is to increase the necessary energy needed to destroy disease-causing pathogens, and when properly combined, it can dramatically improve patients' general wellbeing. In this study, we used intravenously injected C-BSA in the tail to replicate the MN model. The UTP of rats significantly increased, which is one of the indicators of a successful model. Significant IgG buildup was seen by immunofluorescence in the capillary collaterals of the kidney, and the glomerular basement membrane was thickened by electron microscopy. Along with extensive fusion or detachment of peduncles, there was also a significant buildup of electron-dense materials beneath the epithelium. An imbalance between oxidation and antioxidant defense mechanisms can result in oxidative stress, which in turn generates significant amounts of reactive oxygen and lipid peroxidation byproducts. The heightened oxidative stress can damage cells and trigger apoptosis, potentially occurring at various stages of disease progression. Renal fibrosis has been closely associated with oxidative stress, wherein the peroxidative stimulus resulting from oxidative stress can facilitate the accumulation of ECM and expedite renal fibrosis. The production of ROS can be promoted by NOX4, and the abundance of ROS can activate multiple signaling pathways implicated in renal fibrosis, including TGF-β1/Smads, thereby accelerating the renal fibrosis process (He *et al*., 2016).

A small molecular G protein (rac1 or rac2), two cytosolic subunits (gp91phox and p22phox), and

three cytoplasmic subunits (p67-phox, p47-phox, and p40-phox) make up NADPH oxidase, a major source of ROS. Nox4 is one of the several subtypes of NADPH oxidase (Muñoz *et al*., 2020). These subtypes are prevalent in renal tissue and are important ROS producers in the kidney. As a secondary messenger, ROS interacts either directly or indirectly with protein kinases and protein phosphatases, affecting cellular functions like cell division, proliferation, and death as well as other biological processes. Collagen, an essential protein and fibrous component of connective tissue, is produced and secreted by fibroblasts. A key role is played by collagen-I, a crucial protein that makes up the ECM and intercellular matrix in connective tissue. It stimulates fibroblast proliferation and collagen and fibronectin synthesis under the control of TGF-1, which ultimately leads to ECM fibrosis (Yang, 2019). The results of this study show that the MN Group had higher expression levels of renal fibrosis markers such as TGF-1, Collagen-I, and α-SMA. However, after being administered the YSTLF, these expressions reduced in the YSTLF Group and BNPL Group, indicating that the YSTLF significantly improved renal fibrosis in rats with MN. Nrf2 is a crucial regulator of the body's natural antioxidant defense mechanism. The activation of the Nrf2 signaling pathway is essential for controlling the transcription of numerous proteins involved in antioxidant functions. Normally, Nrf2 binds to a protein called Kelch's ECH-associated protein 1 (Keap1) in the cytoplasm. However, when oxidative stress occurs, Nrf2 becomes activated and moves from the cytoplasm to the nucleus. In the nucleus, it binds to the antioxidant response element (ARE), which regulates the expression of antioxidant enzymes (Dong *et al*., 2019). Binding to HO-1, an enzyme, can enhance the production of bilirubin, a potent antioxidant (Liu *et al*., 2019). Thus, the Nrf2/HO-1 pathway plays a crucial role in protecting against oxidative stress and serves as an important self-protection system in the body.

SOD is a type of active enzyme that contains metal elements and functions as a significant antioxidant in the body. Its activity indirectly indicates the body's ability to combat oxidative stress (Policar *et al*., 2022) and protect tissues. In this study, the level of SOD was used as an indicator to assess tissue antioxidant capacity.

MDA is a byproduct of lipid peroxidation caused by oxygen free radicals and is commonly used as an indicator of oxidative stress. The study results indicated that compared to the NC Group, rats in the MN Group exhibited increased expression of renal oxidative stress markers, including Nrf2, HO-1, NOX4, and MDA, while SOD expression decreased, suggesting the presence of oxidative stress in the kidneys of rats with MN. However, the compensatory anti-oxidative stress level increased.

In the YSTLF Group and BNPL Group, the expressions of Nrf2 and HO-1, which can intervene in rat kidneys, were higher compared to the MN Group. Additionally, the serum SOD expression was significantly higher, and the serum MDA expression decreased compared to the MN Group. The expression of NOX4 increased compared to the NC group, and NOX4 may further influence Nrf2/HO-1 expression by mediating pro-fibrotic factors. This aspect requires further verification. The results of this study indicated that the YSTLF could activate the expression of the Nrf2/HO-1 pathway in rats with MN, and that it could enhance the anti-oxidative stress level by stimulating Nrf2/HO-1 activation.

CONCLUSION

To sum up, the YSTLF has the potential to reduce renal oxidative stress and fibrosis in rats with MN. Its mechanism of action appears to involve enhancing the renal antioxidant stress level by activating the Nrf2/HO-1 signaling pathway. Additionally, it inhibits renal fibrosis by suppressing renal oxidative stress. Further research is needed to explore additional mechanisms.

FUNDING

This study was supported by Hebei Natural Science Foundation Project (No. 2019423037).

REFERENCES

Beck LH, Salant DJ. 2014. Membranous nephropathy: From models to man. **J Clin Inv** 124: 2307 - 2314. **https://doi.org/10.1172/JCI72270**

Border WA, Ward HJ, Kamil ES, Cohen AH. 1982. Inducion of membranous nephropathy in rabbits by administration of an exogenous cationic antigen. **J Clin Inv** 69: 451 - 461. **https://doi.org/10.1172/JCI110469**

Burbelo PD, Joshi M, Chaturvedi A, Little DJ, Thurlow JS, Waldman M, Olson SW. 2020. Detection of PLA2R autoantibodies before the diagnosis of membranous nephropathy. **J Am Soc Nephrol** 31: 208 - 217.

https://doi.org/10.1681/ASN.2019050538

Chen SZ, Zang QN, Zhang Z, Song RJ, Tan JC. 2018. Effect of Yishen Tongluo Formula on kidney protection and podocyte skeleton related proteins in rats with membranous nephropathy. **Chin Tradit Herb Drugs** 49: 4857 - 4863.

Chen X, Song L, Hou Y, Li F. 2019. Reactive oxygen species induced by icaritin promote DNA strand breaks and apoptosis in human cervical cancer cells. **Oncol Rep** 41: 765 - 778. **https://doi.org/10.3892/or.2018.6864**

Chen YX, Dai Y, Xia J, Liu J, Zhou G, Chen C, Jiang B, Yin L, Li G. 2022. Serum pharmacochemistry combining network pharmacology to discover the active constituents and effect of Xijiao Dihuang Tang prescription for treatment of blood-heat and blood-stasis syndrome-related disease. **Oxid Med Cell Longev** 7: 6934812. **https://doi.org/10.1155/2022/6934812**

Curthoys NP, Gstraunthaler G. 2014. pH-responsive, gluconeogenic renal epithelial LLC-PK1-FBPase+cells: a versatile *in vitro* model to study renal proximal tubule metabolism and function. **Am J Physiol Renal Physiol** 307: 1 - 11. **https://doi.org/10.1152/ajprenal.00067.2014**

Dong A, Tan XY, Kong Q, Zhang MZ. 2019. Protective effect and mechanism of Schisandra chinensis extract on oxidative stress in diabetic nephropathy mice. **Chin Trad Herbal Drugs** 50: 6038 - 6044.

Gao L, Zhao JJ, Li YY, Wang TM, Yu KY. 2019. Advances in modern research on the mechanism of action of dilong in the treatment of ischemic stroke. **Lishizhen Med Materia Med Res** 30: 446 - 448.

He T, Xiong J, Nie L, Yu Y, Guan X, Xu X, Xiao T, Yang K, Liu L, Zhang D, Huang Y, Zhang J, Wang J, Sharma K, Zhao J. 2016. Resveratrol inhibits renal interstitial fibrosis in diabetic nephropathy by regulating AMPK/NOX4/ROS pathway. **J Mol Med** 94: 1359 - 1371. **https://doi.org/10.1007/s00109-016-1451-y**

Hoo RL, Wong JY, Qiao C, Xu A, Xu HX, Lam KSL. 2010. The effective fraction isolated from *Radix astragali* alleviates glucose intolerance, insulin resistance and hypertriglyceridemia in db/db diabetic mice through its anti-inflammatory activity. **Nutr Metab** 7: 1 - 12. **https://doi.org/10.1186/1743-7075-7-67**

Kawakami T, Fujikawa A, Ishiyama YH, Hosojima M, Saito A, Kubota M, Fujimura S, Kadowaki M. 2016. Protective effect of composite earthworm powder against diabetic complications via increased fibrinolytic function and improvement of lipid metabolism in ZDF rats. **Biosci Biotechnol Biochem** 80: 1980 - 1989. **https://doi.org/10.1080/09168451.2016.1166932**

Kim KK, Sheppard D, Chapman HA. 2018. TGF-β1 signaling and tissue fibrosis. **Cold Spring Harb Perspect Biol** 10: a022293. **https://doi.org/10.1101/cshperspect.a022293**

Lei J, He P. 2019. Mechanism and treatment progress of podocyte injury in membranous nephropathy. **Chin J Postgrad Med** 42: 567 - 572.

Li WW, Guo H, Wang XM. 2013. Relationship between endogenous hydrogen sulfide and blood stasis syndrome based on the Qi-blood theory of Chinese medicine. **Chin J Integr Med** 19: 701 - 705. **https://doi.org/10.1007/s11655-013-1567-7**

Li J, Hu R, Xu S, Li Y, Qin Y, Wu Q, Xiao Z. 2017. Xiaochaihutang attenuates liver fibrosis by activation of Nrf2 pathway in rats. **Biomed Pharmacother** 96: 847 - 853. **https://doi.org/10.1016/j.biopha.2017.10.065**

Li XN, Niu P, Zeng JC. 2019. Application of leech powder in the treatment of cerebral infarction patients. **Chin Modern Med** 26: 38 - 40.

Li XL, Zhao TT, Gu JL, Wang Z, Lin J, Wang R, Duan T, Li Z, Dong R, Wang W, Hong KF, Liu Z, Huang W, Gui D, Zhou H, Xu Y. 2022. Intake of flavonoids from *Astragalus membranaceus* ameliorated brain impairment in diabetic mice via modulating brain-gut axis. **Chin Med** 17: 22. **https://doi.org/10.1186/s13020-022-00578-8**

Liu Y, Xu X, Xu R, Zhang S. 2019. Renoprotective effects of isoliquiritin against cationic bovine serum albumin-induced membranous glomerulonephritis in experimental rat model through its anti-oxidative and anti-inflammatory properties. **Drug Des Devel Ther** 13: 3735 - 3751. **https://doi.org/10.2147/DDDT.S213088**

Lu XY, Xu H, Li G, Zhao T. 2014. Study on correspondence between prescription and syndrome and the essence of phlegm and blood stasis syndrome in coronary heart disease based on metabonomics. **Chin J Integr Med** 20: 68 - 71. **https://doi.org/10.1007/s11655-012-1182-z**

Ma CY, Liu JH, Liu JX, Shi DZ, Xu ZY, Wang SP, Jia M, Zhao FH, Jiang YR, Ma Q, Peng HY, Lu Y, Zheng Z, Ren FX. 2017. Relationship between two blood stasis syndromes and inflammatory factors in patients with acute coronary syndrome. **Chin J Integr Med** 23: 845 - 849. **https://doi.org/10.1007/s11655-016-2746-0**

Muñoz M, López-Oliva ME, Rodríguez C, Martínez MP, Sáenz-Medina J, Sánchez A, Climent B, Benedito S,

García-Sacristán A, Rivera L, Hernández M, Prieto D. 2020. Differential contribution of Nox1, Nox2 and Nox4 to kidney vascular oxidative stress and endothelial dysfunction in obesity. **Redox Biol** 28: 1 - 13. **https://doi.org/10.1016/j.redox.2019.101330**

Policar C, Bouvet J, Bertrand HC, Delsuc N. 2022. SOD mimics: From the tool box of the chemists to cellular studies. **Curr Opin Chem Biol** 67: 102109. **https://doi.org/10.1016/j.cbpa.2021.102109**

Ronco P, Beck L, Debiec H, Fervenza FC, Hou FF, Jha V, Sethi S, Tong A, Vivarelli M, Wetzels J. 2021. Membranous nephropathy. **Nat Rev Dis Primers** 7: 69. **https://doi.org/10.1038/s41572-021-00303-z**

Su M, Tang T, Tang WW, Long Y, Wang L. 2023. Astragalus improves intestinal barrier function and immunity by acting on intestinal microbiota to treat T2DM: a research review. **Front Immunol** 14: 1243834. **https://doi.org/10.3389/fimmu.2023.1243834**

Sun YX, Liu JC. 2008. Structural characterization of a water-soluble polysaccharide from the roots of *Codonopsis pilosula* and its immunity activity. **Int J Biol Macromol** 43: 279 - 282.

Sun F, Indran IR, Zhang ZW, Tan MHE, Li Y, Lim ZLR, Hua R, Yang C, Soon FF, Li J, Xu HE, Cheung E, Yong EL. 2015. A novel prostate cancer therapeutic strategy using icaritin-activated arylhydrocarbon-receptor to co-target androgen receptor and its splice variants. **Carcinogenesis** 36: 757 - 768. **https://doi.org/10.1093/carcin/bgv040**

Sun Y, Qin S, Li W, Guo YB, Zhang Y, Meng L, Sun Y, Ji H, Pan Y, Liu X, Hu B, Shu Y, Li Y, Meng Z, Gu K, Guo H, Chen G, Ye B, Meng K, Pi S. 2021. A randomized, double-blinded, phase III study of icaritin versus huachashu as the first-line therapy in biomarker-enriched HBV-related advanced hepatocellular carcinoma with poor conditions: Interim analysis result. **J Clin Oncol** 39 S4077. **https://doi.org/10.1200/jco.2021.39.15_suppl.4077**

van de Logt AE, Fresquet M, Wetzels JF, Brenchley P. 2019. The anti-PLA2R antibody in membranous nephropathy: what we know and what remains a decade after its discovery. **Kidney Int** 96: 1292 - 1302. **https://doi.org/10.1016/j.kint.2019.07.014**

Wang Y, Tang L, Zhou K, Zhang Q. 2015. Effects of gypenosides on RAGE expression and oxidative stress in human mesangial cells induced by AGEs. **Chinese Traditional and Herbal Drugs** 46: 3060 - 3064.

Wang YR, Yang K, Cui WY. 2018. Effect of gypenoflavone on A549 cells damaged by hydrogen peroxide. **China J Chin Materia Med** 43: 1014 - 1020.

Xie F, Sakwiwatkul K, Zhang C, Wang Y, Zhai L, Hu S. 2013. *Atractylodis macrocephalae* Koidz. polysaccharides enhance both serum IgG response and gut mucosal immunity. **Carbohydr Polym** 91: 68 - 73. **https://doi.org/10.1016/j.carbpol.2012.07.083**

Yang CH. 2019. **Comparative study of Rhubarb and TGF-β_1 regulation on the activity of human fibroblasts *in vitro*.** Southwest Medical University.

Yi M, Dai XP, Li QX, Zhao Y, Nie S, Wang D. 2021. 1H - NMR - based metabolomics study on coronary heart disease with blood - stasis syndrome and phlegm syndrome. **Zhong Nan Da Xue Xue Bao Yi Xue Ban** 46: 591 - 600. **https://doi.org/10.11817/j.issn.1672-7347.2021.190172**

Yu G, Wang J. 2016. Susceptible gene polymorphisms for blood stasis syndrome of coronary heart disease. **Chin J Integr Med** 4. **https://doi.org/10.1007/s11655-016-2491-4**

Zhang L, Xu QX, Li Y, Zhao H, Shi X, Peng F, Yu C. 2021. Ameliorative effects of component chinese medicine from *Curcumae rhizoma* and *Sparganii rhizoma*, a traditional herb pair, on uterine leiomyoma in a rat model. **Front Public Health** 28: 674357. **https://doi.org/10.3389/fpubh.2021.674357**

Zhang T, Wang XF, Wang ZC, Lou D, Fang QQ, Hu YY, Zhao WY, Zhang LY, Wu LH, Tan WQ. 2020. Current potential therapeutic strategies targeting the TGF-β/Smad signaling pathway to attenuate keloid and hypertrophic scar formation. **Biomed Pharmacother** 129: 110287. **https://doi.org/10.1016/j.biopha.2020.110287**